Pressure-induced amorphization of $CuFeS_2$ studied by ^{57}Fe nuclear resonant inelastic scattering

Hisao Kobayashi,* Junpei Umemura, Yutaka Kazekami, and Nobuhiko Sakai
Graduate School of Material Science, University of Hyogo, 3-2-1 Koto, Hyogo 678-1297, Japan

Dario Alfè
Department of Earth Sciences and Department of Physics and Astronomy, University of College London, London WC1E 6BT, United Kingdom

Yasuo Ohishi and Yoshitaka Yoda
Japan Synchrotron Radiation Institute, Hyogo 679-5198, Japan

(Received 25 June 2007; revised manuscript received 4 September 2007; published 19 October 2007)

Static and dynamic structural properties of $CuFeS_2$ under high pressure were investigated by x-ray diffraction and ^{57}Fe nuclear resonant inelastic scattering. Using x-ray diffraction, we obtained evidence that a pressure-induced amorphization occurs at about 6.3 GPa, which represents a metal-insulator transition. Although partial phonon densities of states extracted from ^{57}Fe nuclear resonant inelastic scattering spectra are similar in the two phases, the derived thermodynamical parameters show anomaly at the transition. The results of extracted partial phonon densities of states and *ab initio* phonon calculations indicate that this pressure-induced amorphization is caused by anomalous pressure dependences of the lower optical phonon branches and the initial slopes of the transverse acoustic phonon branches.

DOI: 10.1103/PhysRevB.76.134108 PACS number(s): 62.50.+p, 63.20.−e, 61.43.Er, 71.30.+h

I. INTRODUCTION

Electron correlation plays an important role in 3*d* transition-metal compounds since 3*d* electrons tend to be localized in many of these compounds. Thus, the ground state in some of these compounds becomes an antiferromagnetic insulator. The study of metal-insulator (MI) transition in such compounds has arisen as a new subject since the discovery of high-T_c superconductors. This transition is controlled by two different parameters: i) the chemical potential or filling of the *d* band and (ii) the bandwidths (W) of *d* and *p* bands.[1] Hydrostatic pressure is an ideal perturbation of W because W is directly related to the bond length and angle.[2] Pressure-induced MI transitions are often accompanied by structural changes. Spontaneous disordering of crystal structure may occur simultaneously with the MI transition.[3,4]

At ambient pressure, $CuFeS_2$ (chalcopyrite) crystallizes into a body centered tetragonal lattice with space group $I\bar{4}2d$, which is an antiferromagnetic semiconductor with high Néel temperature, T_N=823 K.[5–7] The ordered magnetic moment of the Fe atom is 3.42 μ_B, which is much smaller than that of the free Fe^{3+} ion with a high-spin state.[8] However, recent ^{57}Fe Mössbauer study using many different samples indicates that the extrapolated magnetic hyperfine field, 363 kOe, is comparable with the expected hyperfine field of the Fe^{3+} ion.[9] The results of optical reflectivity and photoemission show that $CuFeS_2$ belongs to a charge-transfer regime.[10,11] Furthermore, the S $3p \rightarrow$ Fe $3d$ charge-transfer energy was estimated to be close to zero. The above results point out that the Fe 3*d* states in $CuFeS_2$ are strongly hybridized with the S 3*p* states.

The room temperature electrical resistivity of $CuFeS_2$ as a function of pressure[12] shows that the resistivity abruptly decreases at 6.5 GPa, corresponding to the MI transition, and there is another small anomaly at 2.8 GPa. As a result of optical refractivity measurements under pressure,[13] the infrared region in the refractivity spectra suddenly increases above 5 GPa and the overall feature of the spectrum above 6.2 GPa becomes different from that in low pressure. High-pressure ^{57}Fe Mössbauer spectroscopy reveals vanishing of the magnetic hyperfine field as well as an abrupt increase in the center shift at about 6.5 GPa.[14] These results show a substantial change in the electronic structure of $CuFeS_2$ at about 6.5 GPa. Meanwhile, the pressure dependences of the refractivity spectra and the hyperfine interaction parameters show no anomaly at 2.8 GPa.[9,13,14]

High-pressure x-ray diffraction measurements[13,15] reveal a first-order phase transition at about 6.5 GPa and room temperature. Above 6.2 GPa, Sato *et al.* observed several very weak diffraction lines using alcohol as a pressure-transmitting medium, which were indexed by a hcp structure.[13] On the other hand, Tinoco *et al.* determined the structure above 7 GPa, which has the one of a disordered rocksalt, from energy dispersive x-ray diffraction patterns using silicon oil as a pressure-transmitting medium.[15] The phase transition at about 6.5 GPa causes simultaneous changes in electrical and structural properties though recent high-pressure resistivity measurement did not show the first-order phase transition at about 6.5 GPa.[9] These results suggest that the physical properties in the high-pressure phase as well as the phase transition strongly depend on a quality of sample as shown in the dependence of the linewidth in the observed Mössbauer spectra versus the magnetic hyperfine field in $CuFeS_2$ at ambient conditions.[9] Thus, there is a need to study the structural properties of $CuFeS_2$ statically and dynamically under pressure using a high-quality sample to gain insight into the mechanism of this phase transition.

A new method based on nuclear resonant inelastic scattering (NRIS) was introduced to measure phonon densities of states (DOS's) in samples containing suitable Mössbauer nuclei in a crystalline or noncrystalline state using synchrotron

radiation.[16–18] It is possible to observe the intrinsic motion of specific isotopes in compounds. Recently, this technique was successfully applied to measure the phonon DOS under high pressure.[19–22]

In this paper, we present evidence of pressure-induced amorphization of $CuFeS_2$ at 6.3 GPa. This result has been obtained by x-ray diffraction measurement using synchrotron radiation under good hydrostatic conditions. The results of ^{57}Fe NRIS and *ab initio* phonon calculations show that the pressure-induced amorphization is due to anomalous pressure dependences of the lower optical phonon branches and the initial slopes of the transverse acoustic phonon branches.

II. EXPERIMENT

Polycrystalline samples enriched with 50 at. % ^{57}Fe were prepared by a method described elsewhere.[14] The samples obtained were analyzed by means of x-ray diffraction and confirmed to be single phase. At ambient conditions, the magnetic hyperfine field of the sample was evaluated to be 364 kOe from a conventional Mössbauer spectrum, which is in very good agreement with the extrapolated one.[9] Thus, the samples have purely stoichiometric compositions and no disorder between Cu and Fe within an experimental accuracy.

The x-ray diffraction data under pressure were collected on the beamline BL10XU at SPring-8, Japan using angle-dispersive techniques and an image-plate detector at room temperature. The incident x-ray wavelength was calibrated to be 0.4133 Å. Finely ground samples were loaded into a diamond anvil cell (DAC) with ruby chips. In previous two x-ray diffraction experiments,[13,15] they observed weak and broad diffraction peaks in patterns and there is a discrepancy between their results of the structure above 6.5 GPa. Since nonhydrostatic stress leads to significant broadening and shifts in the position of diffraction peaks in some case, we used helium as a pressure-transmitting medium to ensure good hydrostatic conditions. The ^{57}Fe NRIS experiments under high pressure were performed on the beamline BL09XU at SPring-8 using a special DAC up to 14 GPa at room temperature.[20,22] The pulsed synchrotron radiation was monochromatized with 3.3 meV resolution by a high-resolution monochromator. The ^{57}Fe NRIS spectra were measured by tuning the highly monochromatized beam in an energy range of about ±80 meV. The powder samples were loaded into a sample cavity of 0.15 mm diameter in a 0.2-mm-thick Be metal gasket with ruby chips and mixtures of Fluorinert FC70-FC77 1:1 as a pressure-transmitting medium. In our previous high-pressure ^{57}Fe Mössbauer experiments,[14] we used Fluorinert as a pressure-transmitting medium. As mentioned in Sec. I, it was found that the center shift shows an abrupt increase at about 6.5 GPa, which indicates the substantial change in the electronic state of Fe in $CuFeS_2$. Thus, the phase transition at 6.5 GPa is confirmed by nuclear resonant experiments with pressure for Fluorinert. Pressure was calibrated at each experimental condition by measuring the wavelength shift of the R_1 luminescence line of the ruby chips.

III. EXPERIMENTAL RESULTS

Figure 1 shows typical integrated x-ray diffraction patterns of $CuFeS_2$ under pressure. All sharp diffraction lines

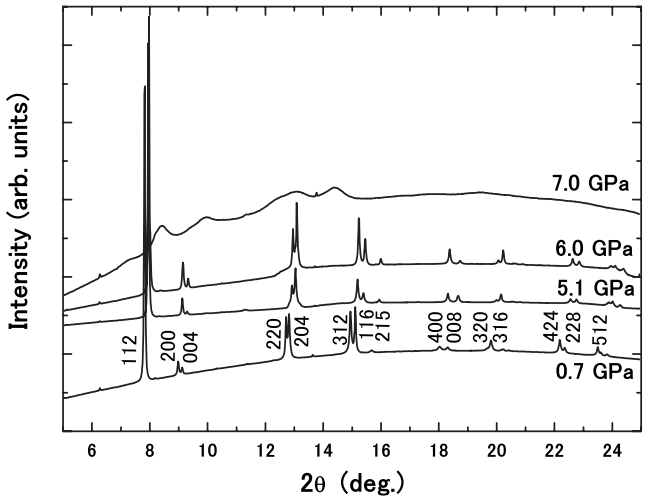

FIG. 1. Typical integrated x-ray diffraction patterns of $CuFeS_2$ with increasing pressure, showing a pressure-induced amorphization at around 6.3 GPa.

observed in the patterns are labeled by the chalcopyrite structure. As seen in Fig. 1, these sharp lines disappear between 6 and 7 GPa and much broader scattering components appear above 6 GPa. These components cannot have been caused by a nonhydrostatic effect because we used helium as the pressure-transmitting medium. Detailed analysis points to the formation of an amorphous phase above 6.3±0.2 GPa. According to electrical resistivity results obtained in previous experimental studies,[12] a drastic decrease in electrical resistivity occurs at 6.5 GPa. Our results strongly suggest that the pressure-induced amorphization corresponds to the MI transition although there is a small discrepancy between the critical pressures P_c. This inconsistency in P_c is most likely caused by the different pressure calibrations used in the present x-ray diffraction and previous electrical resistivity measurements.

Since the diffraction patterns show that the samples in DAC do not completely satisfy the powder conditions, we have refined the cell parameters only from interplanar spacings below P_c. As shown in Fig. 2, volume (V) of $CuFeS_2$ decreases smoothly with pressure. Thus, we observe no anomaly around 2.8 GPa in this compression behavior within an accuracy of the data.

Figure 3 shows typical ^{57}Fe NRIS spectra consisting of large central peaks due to elastic scattering and sidebands resulting from inelastic scattering with the annihilation and creation of phonons. Almost all vibration modes are observed in an energy range of up to 50 meV. The inelastic components in the spectra lead to the Fe partial phonon DOS $[g^e_{\mathrm{Fe}}(E)]$, assuming a harmonic lattice model and considering multiphonon contributions.[23] Application of the sum rule allows calculation of the normalization factors.[24] The extracted $g^e_{\mathrm{Fe}}(E)$ are shown in Fig. 4. Although the features of $g^e_{\mathrm{Fe}}(E)$ at 0.1 MPa, 4.5 GPa, and 14.0 GPa are similar, the widths of the peaks around 10 and 20 meV are broader at 14.0 GPa than those at 0.1 MPa and 4.5 GPa. A spectrum of phonon DOS is typically shifted to higher energies with increasing pressure because of volume reduction. Thus, it is noteworthy

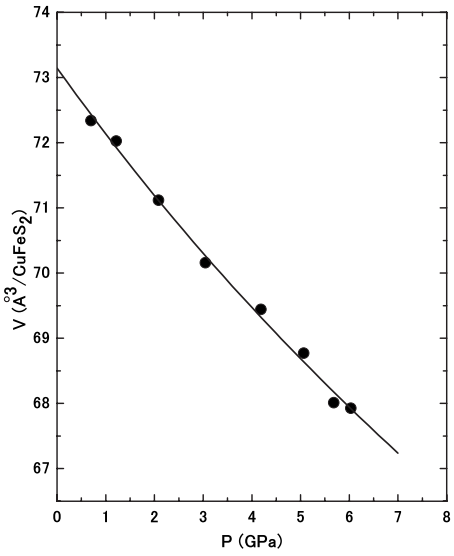

FIG. 2. Pressure dependence of volume (V) in $CuFeS_2$ up to 6.2 GPa. The solid line represents the fitting result based on the Birch-Murnaghan equation.

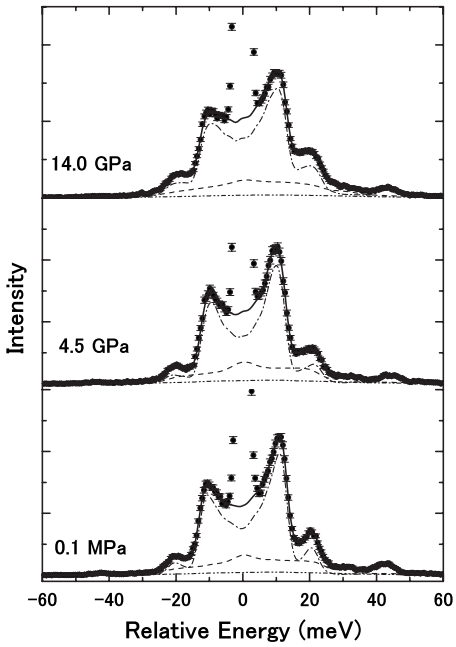

FIG. 3. Typical ^{57}Fe NRIS spectra of $CuFeS_2$ at 0.1 MPa, 4.5 GPa, and 14.0 GPa. The circles with error bars indicate the observed spectra and the solid lines represent the calculated inelastic components. The dashed-and-dotted lines show the single phonon contribution subspectra and the other two lines show two phonon and multiphonon contribution subspectra.

that the peak at around 10 meV in $g^e_{\mathrm{Fe}}(E)$ stays almost unchanged up to 6.0 GPa.

IV. DISCUSSION

The bulk modulus (B) was evaluated based on a Birch-Murnaghan equation:

$$P = \frac{B}{B'}\left[\left(\frac{V_0}{V}\right)^{B'} - 1\right], \tag{1}$$

where V_0 is the ambient-pressure volume and B' is the pressure derivative of B. The solid line in Fig. 2 represents the best fitting curve obtained below 6.3 GPa and the refined B value is 69.9±0.7 GPa with $B'=4$. This refined B value is 1.3 times smaller than that estimated with $B'=4$ from previous compression behavior[15] and is comparable with that of FeS in a troilite phase with an energy gap caused by strong electronic correlation.[25,26]

The mean recoilless fraction ($\overline{f_{\mathrm{LM}}}$) and the mean force constant ($\overline{D_{\mathrm{Fe}}}$) of the resonant ^{57}Fe nuclei were derived from the zero- and third-order moments of the normalized experimental data, respectively.[24] The pressure dependences of $\overline{f_{\mathrm{LM}}}$ and $\overline{D_{\mathrm{Fe}}}$ show anomalies at P_c as seen in Figs. 5(a) and 5(b), while the feature of $g^e_{\mathrm{Fe}}(E)$ above P_c is similar to those below P_c. Given that $\overline{f_{\mathrm{LM}}}$ generally increases with increasing pressure, it can be said that the pressure dependence of $\overline{f_{\mathrm{LM}}}$ below P_c, where $\overline{f_{\mathrm{LM}}}$ decreases with pressure, is anomalous. The mean squared thermal displacement ($\overline{\Delta x^2}$) on an Fe atom was estimated from $\overline{f_{\mathrm{LM}}}$ according to the relation

$$\overline{f_{\mathrm{LM}}} = \exp(-k^2\overline{\Delta x^2_{\mathrm{Fe}}}), \tag{2}$$

with $k=7.304$ Å^{-1} as the wave vector of 14.413 keV γ ray. The results are shown in Fig. 5(c). With increasing pressure, $\overline{\Delta x^2_{\mathrm{Fe}}}$ increases up to 6 GPa and decreases above 8 GPa. These pressure dependences reveal some softening in the lattice vibration modes of the Fe atom with pressure up to P_c.

There is a simple scaling law between $g^e_{\mathrm{Fe}}(E)$ and the total phonon DOS in the low-energy region where a material shows a Debye-like vibration behavior.[27] For a polycrystalline sample, $g^e_{\mathrm{Fe}}(E)$ can be described by

$$g^e_{\mathrm{Fe}}(E) = \left(\frac{m_N}{\bar{M}}\right)\frac{E^2}{2\pi^2\hbar^3\rho\overline{v_D}^3} \tag{3}$$

in the low-energy region, where $\overline{v_D}$ represents the average sound velocity of the sample, m_N is the mass of the nuclear resonant isotope, and $\bar{M}$ and ρ are the average atomic mass and density of the atoms of the sample, respectively. It is confirmed that the $g^e_{\mathrm{Fe}}(E) \propto E^2$ relation holds up to about 4.5 meV. The ρ value was estimated from the pressure dependence of V obtained by the present x-ray diffraction measurements. The derived $\overline{v_D}$ values below P_c are shown in Fig. 5(d). Usually, $\overline{v_D}$ increases with pressure because of volume reduction. However, these values indicate almost no pressure dependence.

Ab initio calculations were performed based on density-functional theory (DFT) within the generalized gradient approximation (GGA) to determine the partial phonon DOS's $[g^c(E)]$ of $CuFeS_2$ at the same pressures using the projector augmented wave approach. Calculations were performed using the VASP code.[28] The projector augmented wave potentials of Cu, Fe, and S were taken from the VASP library and had core radii of 2.3, 2.2, and 1.9 a.u., respectively. Full

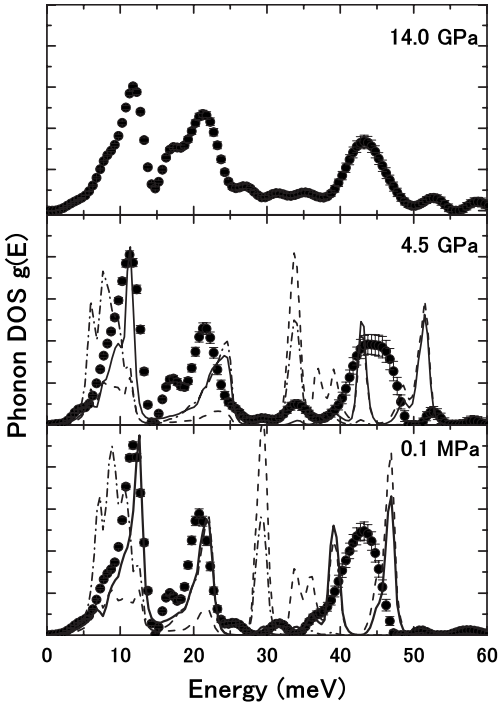

FIG. 4. Partial phonon densities of states $[g(E)]$ of $CuFeS_2$. The circles with error bars represent $g^e_{Fe}(E)$ extracted from ^{57}Fe NRIS spectra at 0.1 MPa, 4.5 GPa, and 14.0 GPa. The dashed-and-dotted, solid, and broken lines indicate the calculated $g^c(E)$ of the Cu, Fe, and S atoms, respectively.

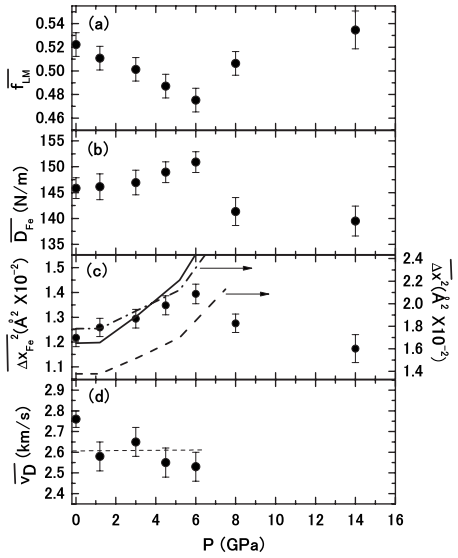

FIG. 5. Variation of the estimated thermodynamical parameters as a function of pressure: (a) mean recoilless fraction ($\overline{f_{LM}}$), (b) mean force constant ($\overline{D_{Fe}}$) of the Fe atom, (c) mean squared thermal displacement ($\overline{\Delta x^2}$), and (d) average sound velocity ($\overline{v_D}$). The dashed-and-dotted, solid, and dashed lines in (c) indicate the calculated $\overline{\Delta x^2}$ from $g^c(E)$ for the Cu, Fe, and S atoms, respectively. The broken line in (d) is guide for the eye.

relativistic effects were included in the potentials. We used a plane wave cutoff of 293 eV, and integration in the Brillouin zone was performed with $2\times2\times2$ and $3\times3\times3$ Monkhorst Pack grids,[29] which gave essentially identical results. Spin polarization was included in all calculations, and antiferromagnetic ordering was found on the Fe atoms.

We calculated the force constant matrix and then the phonon frequencies of $CuFeS_2$ with the chalcopyrite structure using our implementation of the small displacement method.[30] The calculations were performed using supercells containing 64 atoms, and we checked convergence of the results using cells containing up to 216 atoms. We used displacement amplitudes of 0.02 Å, which we found to be small enough to ensure that the calculations were performed in the harmonic regime.

The spectra of $g^c(E)$ are shown in Fig. 4. The large peaks below 30 meV in $g^c_{Fe}(E)$ qualitatively correspond to those in $g^c_{Fe}(E)$ within the experimental resolution. Furthermore, the shapes of these peaks in $g^c_{Fe}(E)$ very much resemble those in $g^e_{Fe}(E)$. In the high-energy region around 40 meV, there is one peak in $g^e_{Fe}(E)$, while there are two sharp peaks in $g^c_{Fe}(E)$. We observe that the DFT-GGA technique employed for the present calculations does not predict the correct electronic structure of $CuFeS_2$ at low pressure, which is a semiconductor due to strong electronic correlation but is predicted to be a metal (though with a very small value of the density of states at the Fermi energy). This inconsistency is due to the well known inaccurate DFT description of strongly correlated systems and may be the reason of the observed differences in the high-energy region of $g_{Fe}(E)$.

As seen in Fig. 4, the peak at around 10 meV in $g^c_{Fe}(E)$ shifts to lower energies with increasing pressure, which qualitatively reflects the pressure dependence of the lowest peak in $g^e_{Fe}(E)$. The spectra of $g^c_{Cu}(E)$ below 10 meV are much larger than those of $g^c_{Fe}(E)$ and $g^e_{Fe}(E)$. Three peaks below 10 meV in $g^c_{Cu}(E)$ also shift to lower energies with increasing pressure. The phonon modes related to S atoms are mainly above 25 meV although the projection of the total phonon DOS onto S atoms is never zero even in the low-energy region.

The $\overline{\Delta x^2}$ values on the Cu, Fe, and S atoms were evaluated from $g^c(E)$ according to the relation

$$\overline{\Delta x^2} = \frac{\hbar^2}{2M}\int_0^\infty \frac{g^c(E)}{E}\coth(\beta E/2)dE, \tag{4}$$

where $\beta=\frac{1}{k_B T}$, k_B is the Boltzmann constant, T is the temperature, and M is the atomic mass. The pressure dependence of $\overline{\Delta x^2_{Fe}}$ estimated from $g^c_{Fe}(E)$ qualitatively agrees with those obtained from $\overline{f_{LM}}$ as seen in Fig. 5(c). The $\overline{\Delta x^2_{Cu}}$ and $\overline{\Delta x^2_S}$ values also increase with pressure up to P_c. The integral in Eq. (4) will be mainly determined by the values of $g^c(E)$ in the low-energy region. Thus, the increases in $\overline{\Delta x^2_{Fe}}$, $\overline{\Delta x^2_{Cu}}$, and $\overline{\Delta x^2_S}$ are caused by the anomalous pressure dependences of $g^e_{Fe}(E)$ and $g^c(E)$ below 15 meV.

Our calculations confirm that $g(E)$ below about 15 meV with the chalcopyrite structure originates from three acoustic and six optical phonon branches. These optical phonon branches are almost flat with wave vectors. The longitudinal acoustic phonon branch crosses these optical phonon

branches at around halfway to a Brillouin zone (BZ) boundary, where the acoustic phonon branch and three of the six optical phonon branches are mixed. Meanwhile, two transverse acoustic phonon branches are reached at energies comparable to those of the optical phonon branches in the BZ boundary vicinity.

Our calculation results under pressure reveal that these optical phonon branches occur in the energy range between 10 and 13 meV at ambient pressure and fall to the range between 7.5 and 10 meV at 7.5 GPa, while the energies of all other optical phonon branches increase with pressure. The initial slopes of the longitudinal acoustic phonon branch at the Γ point in BZ along the symmetrical axes increase with pressure, while those of the transverse acoustic phonon branches decrease. Thus, the pressure-induced amorphization in $CuFeS_2$ is most likely caused by the anomalous pressure dependences of the lower six optical phonon branches and the initial slopes of the transverse acoustic phonon branches at the Γ point.

V. CONCLUSION

We have investigated the structural properties of a high-quality $CuFeS_2$ compound statically and dynamically under high pressure by x-ray diffraction and ^{57}Fe NRIS using synchrotron radiation. The pressure dependence of x-ray diffraction patterns indicates that the pressure-induced amorphization occurs at P_c which corresponds to the MI transition. No anomaly is observed at 2.8 GPa in the pressure dependence of V.

The $g^e_{\mathrm{Fe}}(E)$ were extracted from the observed ^{57}Fe NRIS spectra and f_{LM} and D_{Fe} were derived from the normalized NRIS spectra. The features of $g^e_{\mathrm{Fe}}(E)$ are similar below and above P_c. However, anomalous pressure dependences are observed in $g^e_{\mathrm{Fe}}(E)$ and f_{LM} below P_c, that is, the peak at around 10 meV in $g^e_{\mathrm{Fe}}(E)$ stays almost unchanged and f_{LM} decreases with pressure up to 6.0 GPa. The results of *ab initio* phonon calculations reveal that these anomalous pressure dependences come from the decrease in energies of the six lower optical phonon branches and the initial slopes of the longitudinal acoustic phonon branch below 6.3 GPa with increasing pressure. We conclude that these anomalous pressure dependences cause the pressure-induced amorphization at P_c.

ACKNOWLEDGMENTS

These experiments were performed at SPring-8 with the approval of Japan Synchrotron Radiation Research Institute (JASRI) (Proposal Nos. 2004A0514-ND2a-np and 2003B0099-ND3b-np). H.K. acknowledges the support by the Japanese Ministry of Education, Culture, Sports, Science and Technology and Grant-in-Aid for Scientific Research (c) (5540319). The work of D.A. was conducted as part of a EURYI scheme award as provided by EPSRC (see www.esf.org/euryi).

*kobayash@sci.u-hyogo.ac.jp

[1] See M. Imada, A. Fujimori, and Y. Tokura, Rev. Mod. Phys. **70**, 1211 (1998), and references therein.
[2] W. A. Harrison, *Electronic Structure and the Properties of Solids* (Dover, New York, 1988).
[3] N. Hamaya, K. Sato, K. Usui-Watanabe, K. Fuchizaki, Y. Fujii, and Y. Ohishi, Phys. Rev. Lett. **79**, 4597 (1997).
[4] V. V. Brazhkin and A. G. Lyapin, High Press. Res. **15**, 9 (1996).
[5] T. Teranishi, J. Phys. Soc. Jpn. **16**, 1881 (1961).
[6] M. DiGiuseppe, J. Steger, A. Wold, and E. Kostiner, Inorg. Chem. **13**, 1828 (1974).
[7] H. N. Ok and Ch. S. Kim, Nuovo Cimento Soc. Ital. Fis., B **28B**, 138 (1975).
[8] J. C. Woolley, A.-M. Lamarche, G. Lamarche, M. Quintero, I. P. Swainson, and T. M. Holden, J. Magn. Magn. Mater. **162**, 347 (1996).
[9] C. Boekema, A. M. Krupski, M. Varasteh, K. Parvin, F. van Til, F. van der Woude, and G. A. Sawatzky, J. Magn. Magn. Mater. **272-276**, 559 (2004).
[10] T. Oguchi, K. Sato, and T. Teranishi, J. Phys. Soc. Jpn. **48**, 123 (1980).
[11] M. Fujisawa, S. Suga, T. Mizokawa, A. Fujimori, and K. Sato, Phys. Rev. B **49**, 7155 (1994).
[12] G. M. Pitt and M. K. R. Vyas, Solid State Commun. **15**, 899 (1974).
[13] K. Sato, H. Takahashi, N. Mori, and S. Minomura, Prog. Cryst. Growth Charact. **10**, 125 (1984).
[14] H. Kobayashi, H. Onodera, and T. Kamimura, Hyperfine Interact. **5**, 165 (2002).
[15] T. Tinoco, J. P. Itie, A. Polian, A. S. Miguel, E. Moya, P. Grima, J. Gonzalez, and F. Gonzalez, J. Phys. IV **C9**, 151 (1994).
[16] M. Seto, Y. Yoda, S. Kikuta, X. W. Zhang, and M. Ando, Phys. Rev. Lett. **74**, 3828 (1995).
[17] W. Sturhahn, T. S. Toellner, E. E. Alp, X. W. Zhang, M. Ando, Y. Yoda, S. Kikuta, M. Seto, C. W. Kimball, and B. Dabrowski, Phys. Rev. Lett. **74**, 3832 (1995).
[18] A. I. Chumakov, I. Sergueev, U. van Bürck, W. Schirmacher, T. Asthalter, R. Rüffer, O. Leupold, and W. Petry, Phys. Rev. Lett. **92**, 245508 (2004).
[19] R. Lübbers, H. G. Grünsteudel, A. I. Chumakov, and G. Wortmann, Science **287**, 1250 (2000).
[20] H. K. Mao, J. Xu, V. V. Struzhkin, J. Shu, R. J. Hemly, W. Sturhahn, M. Y. Hu, E. E. Alp, L. Vocadlo, D. Alfè, G. D. Price, M. J. Gillan, M. Schwoerer-Böhning, D. Häusermann, P. Eng, G. Shen, H. Giefers, R. Lübbers, and G. Wortmann, Science **292**, 914 (2001).
[21] V. V. Struzhkin, H. K. Mao, J. Hu, M. Schwoerer-Böhning, J. Shu, R. J. Hemly, W. Sturhahn, M. Y. Hu, E. E. Alp, P. Eng, and G. Shen, Phys. Rev. Lett. **87**, 255501 (2001).
[22] H. Kobayashi, T. Kamimura, D. Alfè, W. Sturhahn, J. Zhao, and E. E. Alp, Phys. Rev. Lett. **93**, 195503 (2004).
[23] H. Kobayashi, Y. Yoda, M. Shirakawa, and A. Ochiai, J. Phys. Soc. Jpn. **75**, 034602 (2006).
[24] H. J. Lipkin, Phys. Rev. B **52**, 10073 (1995).

[25] T. Kamimura, M. Sato, H. Takahashi, N. Môri, H. Yoshida, and T. Kaneko, J. Magn. Magn. Mater. **104-107**, 255 (1992).
[26] K. Kusaba, Y. Syono, T. Kikegawa, and O. Shimomura, J. Phys. Chem. Solids **58**, 241 (1997).
[27] M. Y. Hu, W. Sturhahn, T. S. Toellner, P. D. Mannheim, D. E. Brown, J. Zhao, and E. E. Alp, Phys. Rev. B **67**, 094304 (2006).
[28] G. Kresse and J. Furthmüller, Phys. Rev. B **54**, 11169 (1996).
[29] H. J. Monkhorst and J. D. Pack, Phys. Rev. B **13**, 5188 (1976).
[30] D. Alfè, program available at http://chianti.geol.ucl.ac.uk/~dario